Electronic Supplementary Material (ESI) for Nanoscale.

Electronic Supplementary Information for:

Probing Nano-Patterned Peptide Self-Organisation at the Aqueous Graphene Interface

Z. E. Hughes[a] and T. R. Walsh*[a]

[a] Institute for Frontier Materials, Deakin University, Geelong, VIC 3216, Australia

(33 pages)

Simulation Details

REST Simulations: All simulations were performed using GROMACS version 5.0.[1] The GRAPPA FF[2] was used for the graphene surface with the peptides and water molecules described using the CHARMM22*[3] parameters and the modified version of the TIP3P water model,[4] respectively. The Lennard-Jones non-bonded interactions were tapered to zero between 10.0 and 11.0 Å, while the electrostatic interactions were treated using a particle mesh Ewald summation with a real-space cutoff of 11.0 Å.[5] To ensure robust sampling of the complex energy landscape of these peptides adsorbed at the graphene interface, the Replica Exchange with Solute Tempering (REST)[6] MD simulation approach has been employed throughout. A fuller outline of the REST approach and its implementation can be found in previous studies.[7] In the present work, an effective temperature window of 300-433 K, across which we distributed 16 replicas, was used for each REST simulation. The scaling values, λ, used for the replicas were 0.000, 0.057, 0.114, 0.177, 0.240, 0.310, 0.382, 0.458, 0.528, 0.597, 0.692, 0.750, 0.803, 0.855, 0.930, 1.000. All simulations were performed in the canonical (NVT) ensemble at 300 K and with the temperature regulated via a Nosé-Hoover thermostat.[8] For each replica, an equilibration simulation of 0.5 ns duration was performed, using the appropriately-scaled Hamiltonian, prior to initiating the REST MD simulation, during which time no attempts at exchange between replicas were attempted. Production runs were performed for 20×106 or 50×106 MD steps, for the single chain peptide systems and the peptide over-layer systems, respectively, with exchanges between replicas attempted every 1000 steps (1 ps). A timestep of 1 fs was used for all simulations.

We emphasise here that REST-MD simulations do not alter the thermal temperature of the sample, and instead modify the Hamiltonian for each replica. In our REST-MD simulations, each replica is simulated at a thermal temperature of 300 K. The extent to which the Hamiltonian of each replica is modified is captured by the "effective temperature" (as extensively described by Terakawa *et al*.). We also remark that we have extensive expertise in applying REST-MD simulation to dodecapeptides adsorbed on a range of solid surfaces under aqueous conditions, and have identified this "effective temperature" range based on years of testing and experience. To elaborate, we recognise and understand that the "effective temperature" range used in REST-MD simulations may affect results. In the ideal case, the upper "effective temperature" must be sufficiently high to ensure barriers on the potential energy landscape are crossable. At the same time, the spacing of replicas throughout "effective temperature" space must ensure that the overlap of the potential energies between neighbouring replicas sufficient to confer a reasonable acceptance ratio while also ensuring that the number of replicas is not so high as to either make the replica round trip time too long, or the simulation computationally intractable in terms of computing resource.

Assessing the capability of any bio-interfacial force-field (FF) to reproduce π-π interactions between aromatic side-chains and the graphene surface, under aqueous conditions, is challenging due to the relative paucity of experimental data. Even for those instances when experimental data are available, drawing unambiguous conclusions regarding the comparison between experiment and simulation is non-trivial (for example as discussed in Hughes, Kochandra and Walsh, *Langmuir*, **2017**, 33, 3742). In our case, the GRAPPA force-field was parametrised to reproduce the *in vacuo* adsorption energies of a variety of small organic molecules, including aromatic

molecules (Hughes, Tomasio and Walsh, Nanoscale; Ref 35 in the main text). Furthermore, as discussed herein in the ESI (Section 'Force-Field Comparison'), there was general agreement between the GRAPPA force-field used in the present study and the parameters used by Penna et al. (Ref. 12 in the ESI) regarding the adsorption of the aromatic species. In a previous study (Hughes and Walsh, *J. Mater. Chem. B*, **2014**; Ref 34 in the main text), we calculated the free-energy of adsorption of all twenty amino-acids at the aqueous graphene interface, and we noted reasonable agreement across a range of force-fields that the amino acids with aromatic side-chains were amongst the most strongly-binding amino acids. In summary, there is evidence that the GRAPPA force-field can reasonably reproduce the favourability of aromatic/graphene π-π interactions.

System Setup: In all simulations the peptide chains were modeled in the zwitterionic form (i.e. with no capping groups on the termini) consistent with the peptides used in previously-reported experiments. Glutamic and aspartic acid side-chains were deprotonated, consistent with a pH of 7. For the single chain simulations, each of the five sequences in Table 1 was simulated both when free in solution and when adsorbed at the aqueous graphene interface. Each system comprised a single peptide chain, 6846 water molecules and two Na+ counter-ions. In the simulations of the adsorbed peptide, a graphene sheet, 63.9 × 59.6 Å was used. The dimension of the periodic cell along the direction perpendicular to the graphene surface was set to 57.5 Å. For the simulations of the peptide free in solution, the simulation cell measured 63.9 × 59.6 × 54.0 Å. In the surface-adsorbed case, the length of the periodic cell along the direction perpendicular to the surface plane was set to a value to ensure the density of liquid water in the center of the simulation cell was equal to that of bulk water at ambient temperature and pressure. Similarly, the dimensions of the periodic cell for the simulations of the free peptide (in the un-adsorbed state) were set to recover bulk water density in the cell. For the single-chain REST-MD simulations, the initial conformation of the peptide in each replica was different, with the sixteen initial configurations covering a range of different secondary structure motifs (e.g. α–helix, β-turn, PPII helix and random coil).

For the over-layer simulations of GrBP5-WT, the simulation consisted of 8 or 12 peptide chains adsorbed on a graphene sheet, 6324 water molecules and 16/24 Na+ counter-ions. The simulation cell measured 63.9 × 59.6 × 57.5 Å. The six most populated distinct conformations of GrBP5-WT in the single-chain adsorbed state (herein denoted i1-i6), identified from the clustering analysis of our single chain REST-MD simulations, were used to construct the initial over-layer configurations. Eight different initial over-layer configurations were constructed. Each configuration featured a different proportion of the six distinct conformations of the individual chains (i1-i6), but the relative population of the six conformations over all eight initial over-layer configurations was such that it was approximately equal to the relative populations of i1-i6 identified from the cluster analysis (i.e. over the eight initial over-layer configurations there were approximately twice as many i1 chains as i2 and i3). Two instances each of the eight initial configurations were then randomly distributed over the sixteen replicas.

In Figures S10-S12, to illustrate the degree of sampling in our simulations we show exemplar replica mobilities through "effective temperature" space as a function of REST-MD simulation steps for the GrBP5-WT sequence adsorbed at the aqueous graphene interface for coverages of 1, 8 and 16 adsorbed peptide chains.

Analysis: The degree of residue-surface contact was determined by calculating the fraction of the total reference trajectory (i.e. the baseline trajectory that corresponds, to the unscaled Hamiltonian) that a pre-determined reference site on each residue was found within a cut-off distance with respect to the graphene surface. The cutoffs were assigned on the basis of previous work and inspection of the distance distribution profiles.[7c] The reference sites and cutoff distances are provided in Table S12.

To characterize the Boltzmann-weighted ensemble of peptide conformations at 300 K, the Daura clustering algorithm was performed over the reference trajectory,[9] using a 2.0 Å cutoff for positions of the atoms in the peptide backbone of each chain. The percentage population of each cluster was determined from the fraction of the total number of trajectory frames assigned to that cluster.

The secondary structure of the peptide conformations was analyzed according to two different sets of definitions. In the first scheme, a Ramachandran analysis, secondary structure motifs were assigned on the basis of the ϕ and ψ backbone dihedral angles, with each secondary structure motif corresponding to a range of angles as characterized in previous work.[6b, 7b,c] In the second scheme, secondary structure motifs were assigned on the basis of the definitions within the dictionary of secondary structure of proteins (DSSP) program.[10]

Solvent accessible surface area (SASA) estimates were determined using the double cubic lattice method (DCLM) devised by Eisenhaber et al., using a probe radius of 1.4 Å.[11]

Cluster and Secondary Structure Analysis of Peptide Sequences:
For the single-chain simulations, all five peptide sequences investigated in this work were found to support over 250 distinct conformations (Figure S1). Moreover, no single cluster was dominant, with the most populated peptide conformation accounting for, at most, 15% of the overall ensemble (Table S2). In particular, the GrBP5-M1 and GrBP5-M4 sequences featured an enhanced number of thermally-accessible structures (331 and 360 clusters for M1 and M4 in the un-adsorbed state, respectively) and very flat cluster population distributions (as a function of cluster rank). These broad, flat cluster population distributions, previously seen for another graphene binding peptide sequence,[7c] are indicative of the intrinsically disordered characteristics of these sequences.

Figure S4 shows a representative structure of the most populated cluster for each of the five peptide sequences in solution. For all sequences except GrBP5-M4 these conformations were relatively compact, featuring intra-peptide contacts. In contrast, the most populated cluster of GrBP5-M4 favored a much more extended conformation. Despite the extended conformation of the most populated cluster of GrBP5-M4, analysis of the secondary structure of the peptides showed no meaningful differences in the relative proportions of the different secondary structure motifs between those in GrBP5-M4 and the other four peptide sequences. The secondary structure of the sequences was analyzed according to two methods, one based on a Ramachandran dihedral analysis[6b, 7b,c] and one based on the Dictionary of Secondary Structure of Proteins (DSSP)[10] definitions (see the Simulation Details above for more details). For all five systems, a variety of different secondary structure motifs were predicted to be present

using both definitions (Figure S2), with random coil character accounting for over 70% of the secondary structure (using the DSSP definitions). Overall, in solution the peptides are intrinsically disordered, having a large number of distinct conformations, no dominant conformation(s) and an overall lack of any well-defined secondary structure.

In all cases, the total number of clusters predicted for each peptide sequence adsorbed at the aqueous graphene interface (for the single adsorbed chain systems) was reduced compared to the un-adsorbed case, although the total number of clusters was still high (~170-250 clusters in total), and no single cluster had a population of more than ~13.0 % of the ensemble (Table S3). Again, this signifies IDP character for all five peptide sequences in the adsorbed state. The relative weightings of the different secondary structure motifs of the adsorbed peptides were largely unchanged from those predicted for these sequences in the non-adsorbed state (Figure S4). GrBP5-M1 did show some difference between the adsorbed and solution states, with an increase in the amount of α-helical content present when the peptide was adsorbed (using both definitions of secondary structure analysis). Despite this, using the DSSP definitions of secondary structure random coil was still the dominant trait (greater than 60%) for all sequences. Using the Ramachandran dihedral angles analysis, a mix of different motifs, typically with PPII helix as the single most likely motif, was present for all five sequences. Overall, the intrinsically disordered nature of each peptide sequence, seen in the unadsorbed state, persisted for the adsorbed state. These findings emphasize the need for advanced conformational sampling techniques, such as REST-MD simulations, to ensure the Boltzmann weighted ensemble of conformations of each peptide is sufficiently explored.

Table S1. Degree of residue-surface contact (expressed as a percentage of the number of frames in the reference REST-MD trajectory) between the site in the side-chain of each residue for each peptide sequence and the graphene sheet, for the single adsorbed chain REST-MD simulations.

GrBP5-WT		GrBP5-M1		GrBP5-M2		GrBP5-M4		GrBP5-M5	
Residue	Contact	Residue	Contact	Residue	Contact	Residue	Contact	Residue	Contact
I	9	I	9	I	8	T	17	L	6
M	26	M	47	M	6	Q	57	I	3
V	7	V	45	V	33	S	40	A	4
T	29	T	11	T	27	T	36	T	3
E	7	E	23	E	31	E	13	E	9
S	22	S	46	S	31	S	13	S	19
S	18	S	45	S	35	S	55	S	19
D	12	D	19	D	19	D	7	D	22
Y	79	A	57	W	64	Y	86	Y	77
S	39	S	45	S	41	S	51	S	35
S	32	S	49	S	43	S	48	S	30
Y	81	A	38	W	78	Y	75	Y	68

Table S2. Percentage population of top 10 most populated clusters for each peptide in the un-adsorbed state. Calculated over the full 20 ns REST-MD simulation trajectory.

Cluster	GrBP5-WT	GrBP5-M1	GrBP5-M2	GrBP5-M4	GrBP5-M5
1	15.0	5.3	10.8	3.1	6.2
2	4.4	3.1	4.1	3.1	4.7
3	2.8	3.0	3.4	2.8	4.5
4	2.4	2.9	3.0	2.5	3.7
5	2.4	2.9	2.3	2.2	3.5
6	2.3	2.1	2.0	2.1	2.8
7	2.1	2.1	2.0	2.0	2.5
8	1.8	2.0	2.0	2.0	2.3
9	1.8	2.0	1.9	1.8	1.9
10	1.6	1.9	1.9	1.8	1.8
Total # of conformations	292	331	307	360	311

Table S3. Percentage population of top 10 most populated clusters for each single chain peptide sequence adsorbed at the aqueous graphene interface. Calculated over the full 20 ns REST MD simulation trajectory.

Cluster	GrBP5-WT	GrBP5-M1	GrBP5-M2	GrBP5-M4	GrBP5-M5
1	12.5	9.3	13.1	10.2	6.0
2	7.5	9.1	8.1	7.4	5.3
3	7.4	5.9	6.7	7.4	4.6
4	4.5	4.8	6.1	6.9	4.4
5	4.4	3.6	4.9	5.4	4.0
6	4.3	3.6	4.6	5.0	3.6
7	4.0	3.6	3.8	4.2	3.3
8	3.3	2.3	3.5	3.3	3.3
9	3.0	2.0	2.7	2.9	2.5
10	2.4	1.8	2.5	2.4	2.2
Total # of conformations	192	244	171	175	234

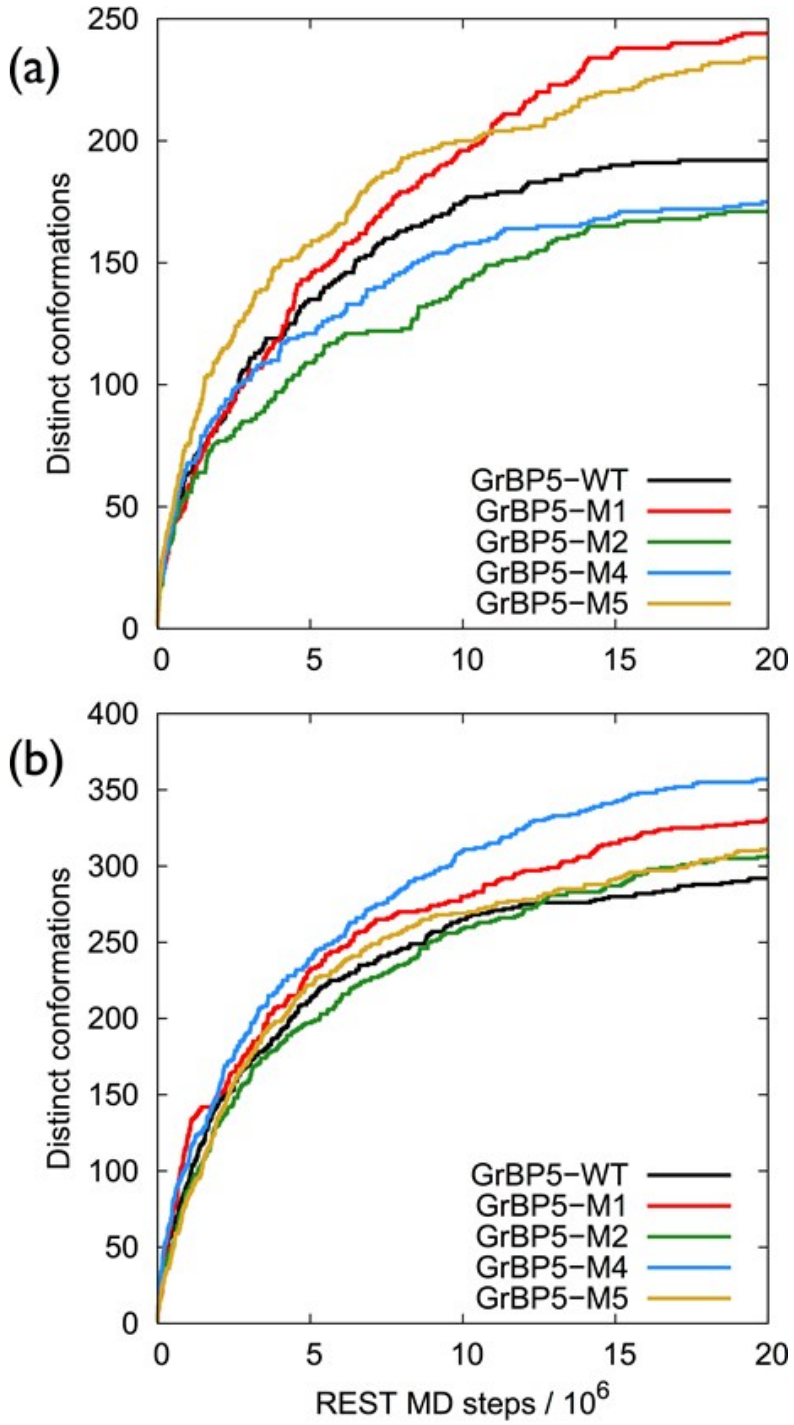

Figure S1. The number of clusters (distinct backbone conformations) identified as a function REST-MD simulation time-steps for the different peptide sequences in (a) the un-adsorbed state and (b) when adsorbed at the aqueous graphene interface.

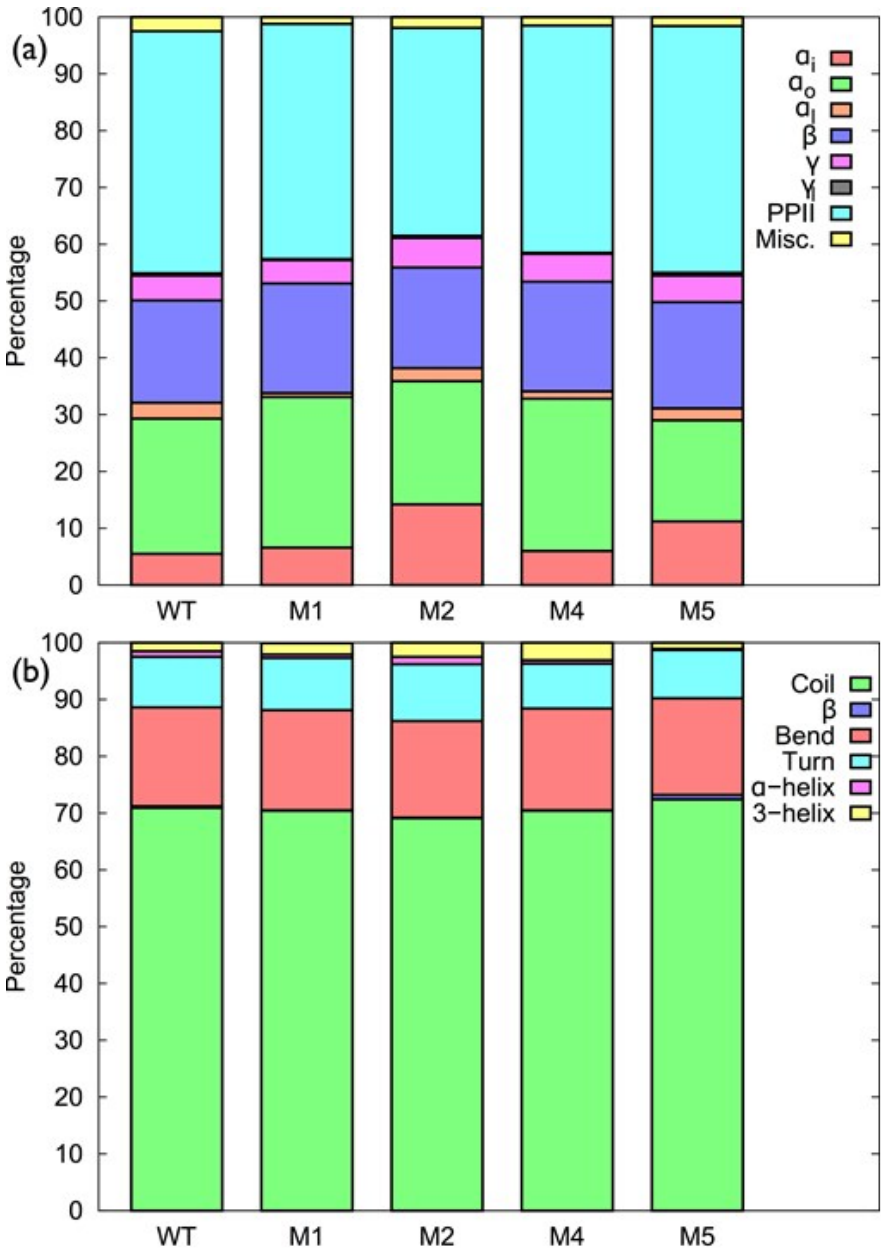

Figure S2. Percentages of different secondary structures motifs identified from the conformational ensemble of peptides in solution, determined by (a) using the DSSP definitions and (b) Ramachandran analysis of the backbone dihedral angles.

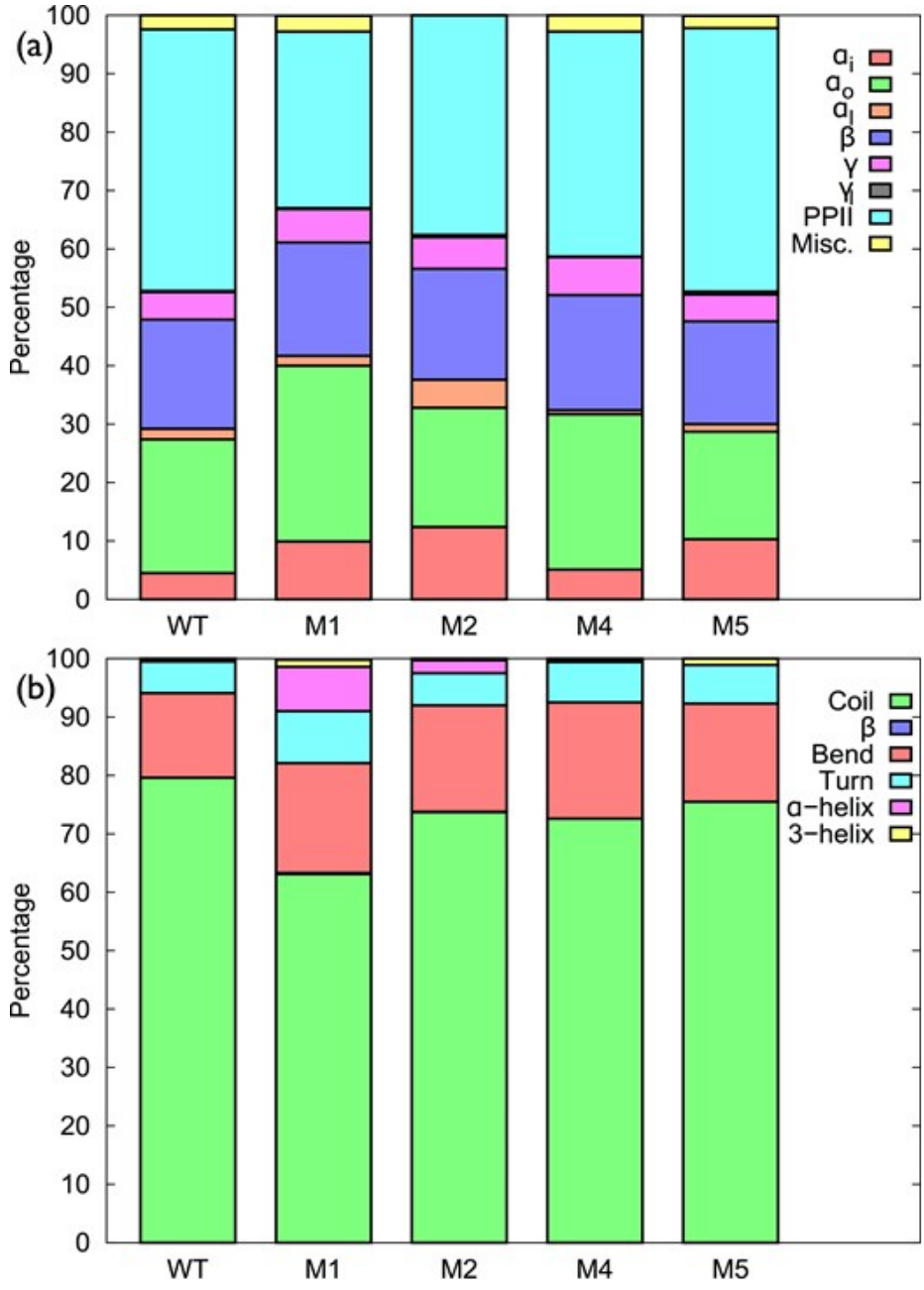

Figure S3. Percentages of different secondary structures motifs identified from the conformational ensemble of peptide chains adsorbed at the aqueous graphene interface (for the single-chain adsorbed case), determined by (a) using the DSSP definitions and (b) Ramachandran analysis of the backbone dihedral angles.

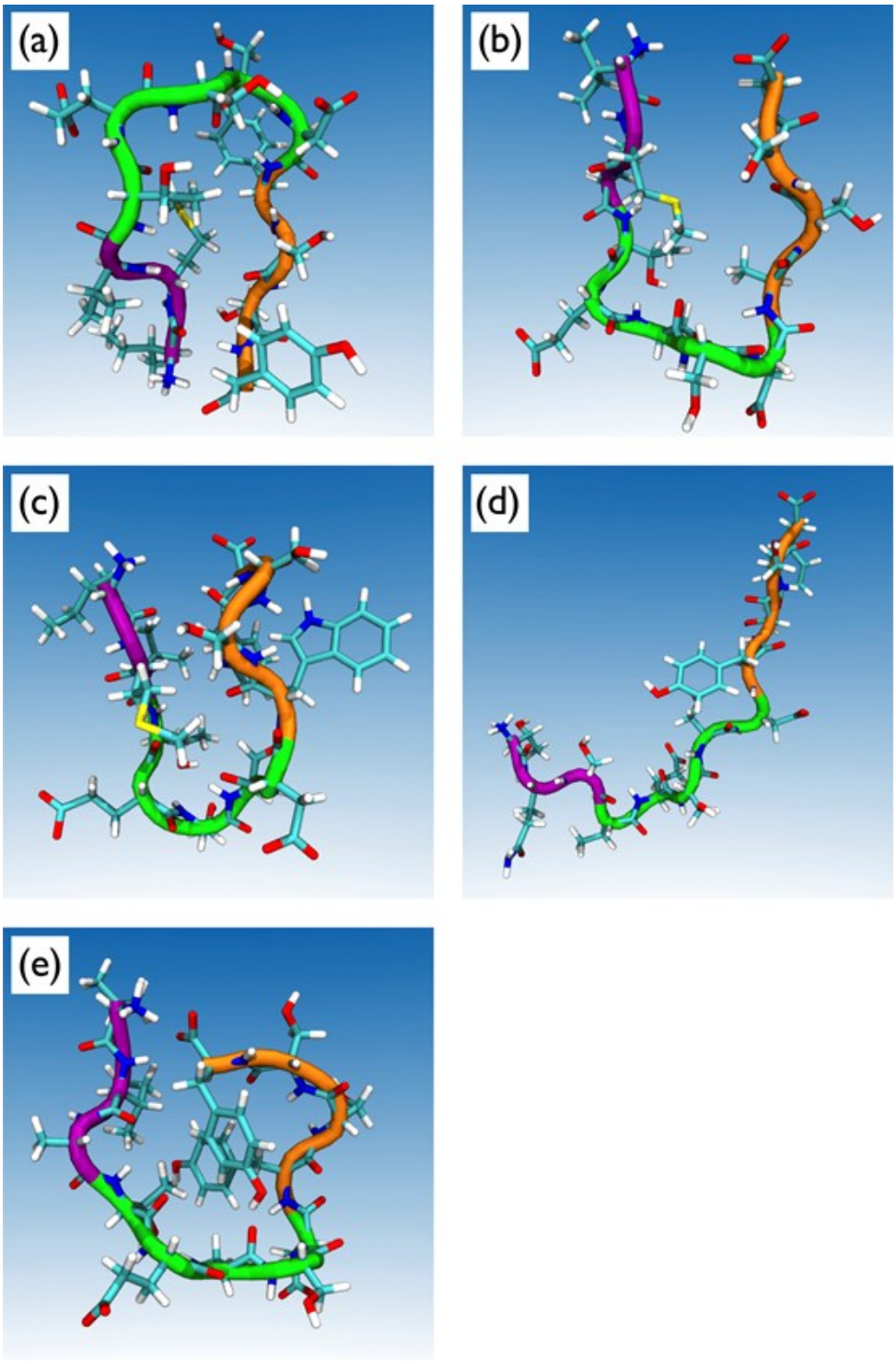

Figure S4. Representative snapshots of most populated clusters of (a) GrBP5-WT, (b) GrBP-M1, (c) GrBP5-M2, (d) GrBP5-M4 and (e) GrBP5-M5 in solution. Water not shown for clarity. The backbone of the peptides are colored by sub-domain: SD1, SD2 and SD3 are purple, green and orange respectively.

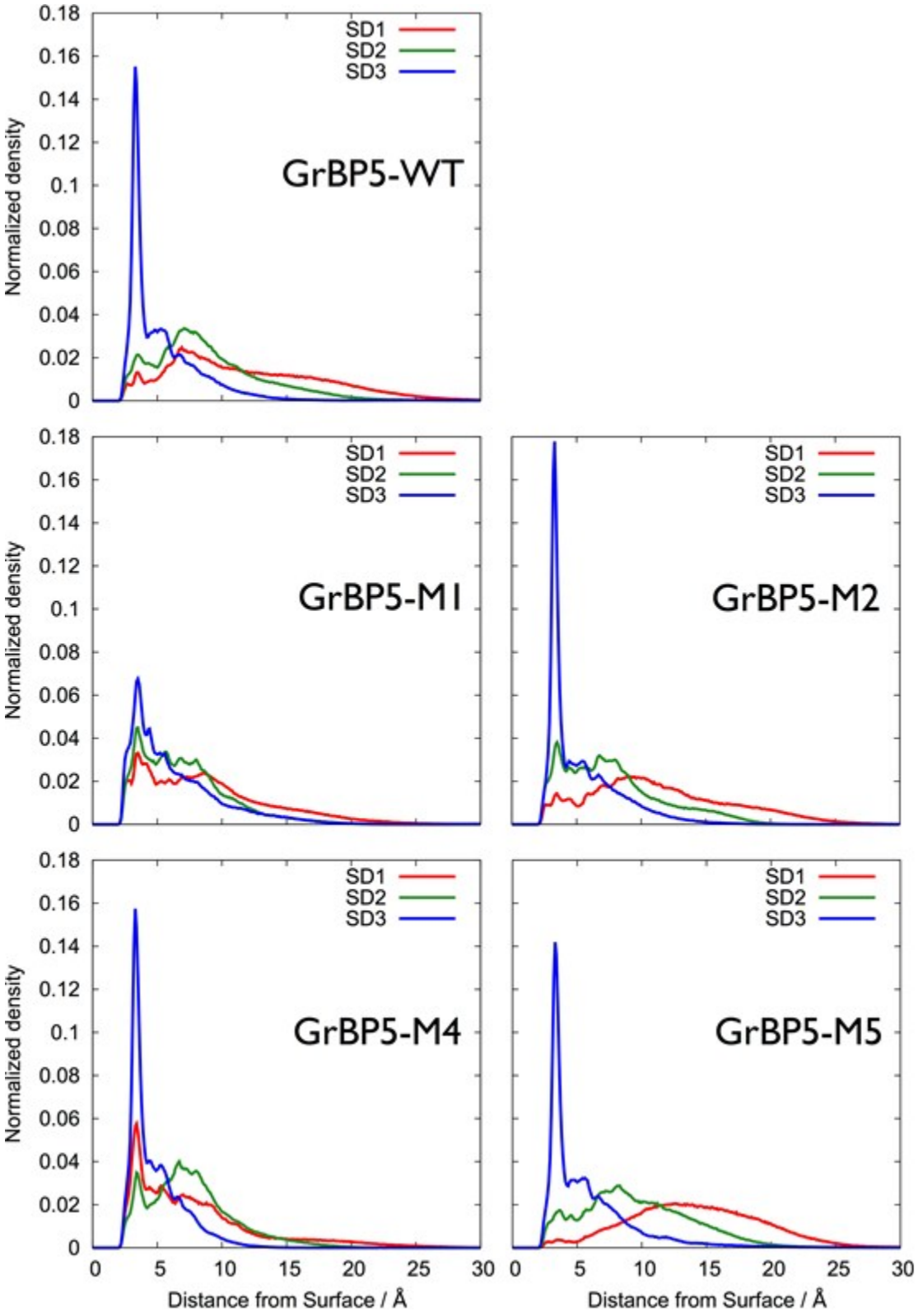

Figure S5. Normalised atom number density profiles of the sub-domains of the different mutant sequences, for the single-chain case of the surface adsorbed peptides.

Table S5. Average degree of direct contact between the site in the side-chain of each residue and the graphene sheet for the GrBP5-WT over-layers, expressed as a percentage of the total frames in the REST-MD trajectory. Data for the single adsorbed peptide chain are also given for comparison.

Residue	Single chain	Eight chains	Twelve chains
I	9	17	11
M	26	25	32
V	7	11	25
T	29	31	22
E	7	4	13
S	22	24	19
S	18	36	25
D	12	12	4
Y	79	93	86
S	39	72	74
S	32	53	51
Y	81	96	87

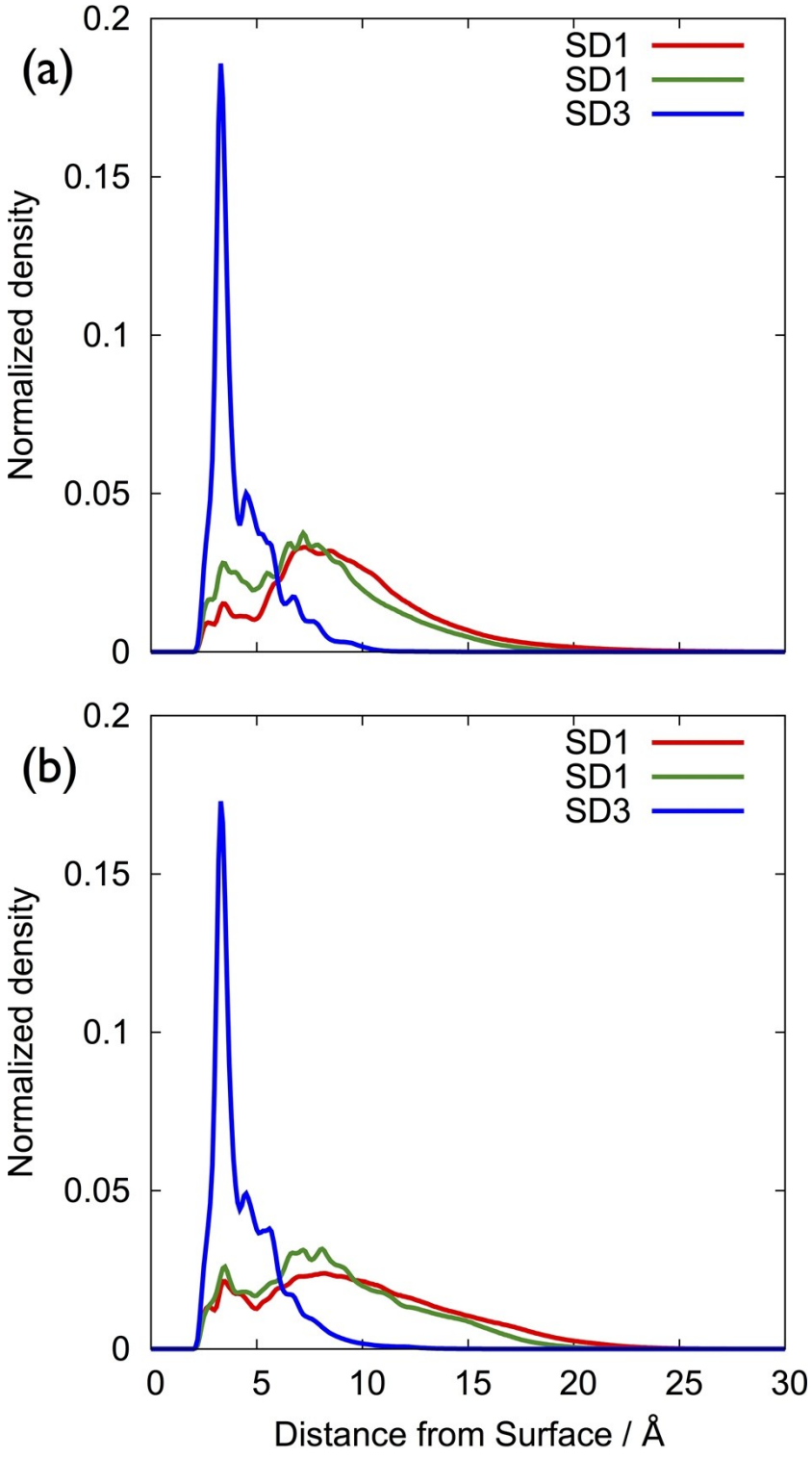

Figure S6. Normalised atom number density profiles of the sub-domains of the over-layers of GrBP5-WT, (a) eight chains and (b) twelve chains.

Table S6. RMSD comparison of the peptide backbone conformational similarity between the top six most populated distinct conformations of the GrBP5-WT peptide adsorbed as a single chain at the graphene interface (*i*1-*i*6) and the top five distinct conformations of each peptide chain in the eight chain over-layer. Conformations were considered a match if the RMSD was ≤ 2 Å.

Single chain conformation	Chain number	Over-layer chain conformation	RMSD [Å]
i1	1	1	1.20
i1	2	2	1.70
i1	2	4	1.05
i1	6	5	0.83
i2	3	1	1.07
i2	4	1	0.99
i2	6	1	1.15
i3	3	2	0.78
i3	5	1	0.54
i4	4	5	1.75
i4	6	2	1.90
i5	6	4	1.37
i6	7	1	1.99
i6	7	3	1.24

Table S7. RMSD comparison of the peptide backbone conformational similarity between the top six most populated distinct conformations of the GrBP5-WT peptide adsorbed as a single chain adsorbed at the graphene interface (*i*1-*i*6) and the top five distinct conformations of each peptide chain in the twelve chain over-layer. Conformations were considered a match if the RMSD was ≤ 2 Å.

Single chain conformation	Chain number	Over-layer chain conformation	RMSD [Å]
i2	2	2	1.26
i2	4	1	1.19
i2	10	2	1.71
i4	1	5	1.99

Table S8. RMSD comparison of peptide backbone conformational similarity between the top two most populated distinct adsorbed conformations of each peptide chain in the eight chain over-layer. Conformations were considered a match if the RMSD was ≤ 2 Å.

Chain number A	Conformation A	Chain number B	Conformation B	RMSD [Å]
3	1	4	1	0.34
3	1	6	1	0.41
3	1	8	1	1.98
4	1	6	1	0.53
6	1	8	1	1.93
1	1	2	2	1.09
3	1	4	2	1.65
4	1	4	2	1.71
5	1	3	2	0.60
6	1	4	2	1.62
7	1	6	2	1.71
8	1	4	2	1.83
4	2	7	2	1.50

Table S9. RMSD comparison of peptide backbone conformational similarity between the top two most populated distinct adsorbed conformations of each peptide chain in the twelve molecule over-layer. Conformations were considered a match if the RMSD was ≤ 2 Å.

Chain number A	Conformation A	Chain number B	Conformation B	RMSD [Å]
4	1	6	1	2.00
4	1	8	1	1.62
2	1	6	2	1.69
4	1	2	2	1.64
4	1	10	2	1.55
8	1	4	2	1.67
8	1	10	2	1.69

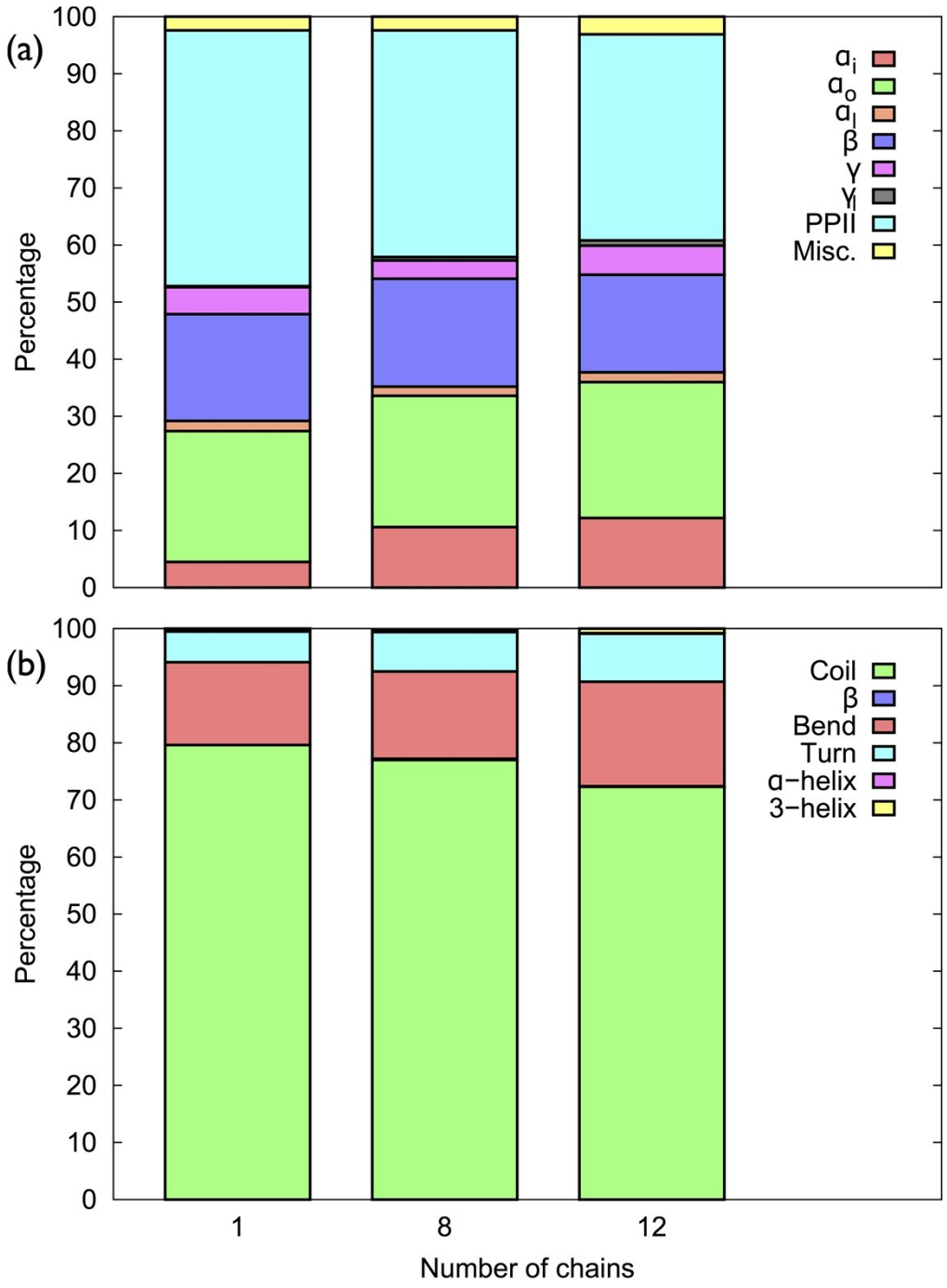

Figure S7. Percentages of different secondary structures motifs identified for GrBP5-WT adsorbed at the aqueous graphene interface as both a single adsorbed chain and as part of an over-layer. Determined by (a) using the DSSP definitions and (b) analysis of the backbone dihedral angles.

Table S10. Number of total, intra- and inter-chain hydrogen bonds per chain, between different sub-domains for the simulations of GrBP5-WT adsorbed at the aqueous graphene interface.

Subdomains	Single chain	Eight chains			Twelve chains		
	Total/Intra-	Total	Intra-	Inter-	Total	Intra-	Inter-
SD1-SD1	0.0±0.1	0.04±0.01	0.01±0.01	0.03±0.02	0.11±0.02	0.02±0.01	0.09±0.02
SD1-SD2	0.1±0.3	0.43±0.03	0.08±0.01	0.35±0.03	0.89±0.02	0.29±0.03	0.60±0.03
SD1-SD3	0.1±0.4	0.40±0.04	0.10±0.05	0.30±0.06	0.40±0.03	0.06±0.03	0.34±0.04
SD2-SD2	0.4±0.6	0.55±0.05	0.43±0.03	0.13±0.06	0.81±0.03	0.63±0.02	0.18±0.04
SD2-SD3	0.6±0.8	1.15±0.03	0.93±0.01	0.23±0.03	1.12±0.03	0.73±0.02	0.38±0.04
SD3-SD3	0.5±0.6	0.91±0.04	0.75±0.01	0.16±0.04	1.05±0.02	0.60±0.01	0.45±0.02
Total	1.7±0.1	3.50±0.06	2.28±0.04	1.23±0.07	4.38±0.03	2.33±0.03	2.05±0.05

Table S11. Breakdown of the percentage of total, intra- and inter-chain hydrogen bonds by different sub-domain pairings, for GrBP5-WT adsorbed at the aqueous graphene interface.

Subdomains	Single chain	Eight chains			Twelve chains		
	Total/Intra-	Total	Intra-	Inter-	Total	Intra-	Inter-
SD1-SD1	0	1	1	2	2	1	4
SD1-SD2	6	12	3	29	20	13	29
SD1-SD3	6	11	4	24	9	3	17
SD2-SD2	24	16	19	10	18	27	9
SD2-SD3	35	33	41	18	26	32	19
SD3-SD3	29	26	33	13	24	26	22
Total	100	100	100	100	100	100	100

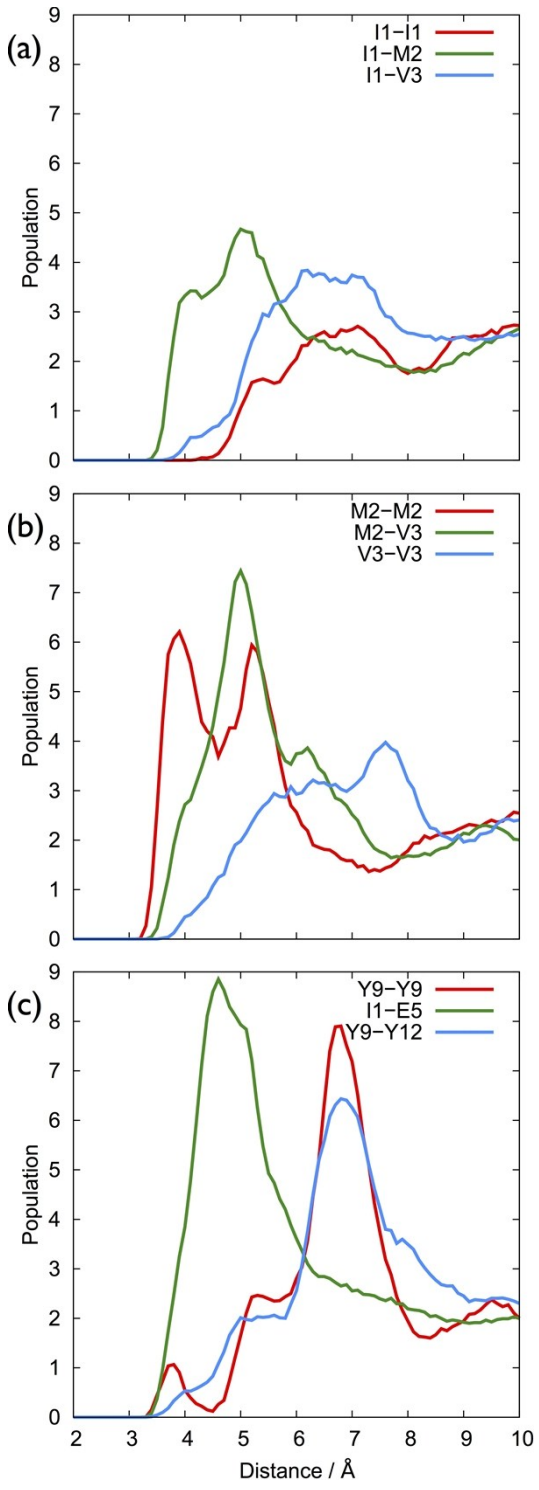

Figure S8. Inter-peptide radial distribution functions of sites in different residues: (a) I1-I1, I1-M2 and I1-V3, (b) M2-M2, M2-V3 and V3-V3 and (c) Y9-Y9, I1-E5 and Y4-Y12.

Table S12. The side-chain site and cutoff distance of each residue used to determine if a residue is in contact with the graphene interface.

Residue	Side-chain site	Cutoff distance [Å]
Ala	β-carbon	5.00
Asp	γ-carbon	5.50
Gln	side-chain N	4.25
Glu	δ-carbon	5.50
Ile	β-carbon	6.00
Leu	γ-carbon	5.50
Met	side-chain S	4.25
Ser	side-chain O	4.25
Thr	side-chain O	4.25
Trp	mid-point of bond between two rings	3.70
Tyr	c.o.m of ring Cs	4.00
Val	β-carbon	5.50

Force-field Comparison

The differences between our work and Penna *et al.* [12] regarding the interaction of SD1 with the substrate may arise from the different force-fields (FFs) used in the two studies. Penna *et al.* calculated the adsorption free-energy profiles for phenol, benzene and butane at the aqueous graphite surface, with minimum values of -17.8, -13.4 and -12.1 kJ mol-1, respectively.[12] Note that minimum values in the free energy profile do not usually correspond with the binding free energy. Previously, we reported adsorption free-energy calculations for all twenty naturally-occurring amino acids, in capped form, to the aqueous graphene interface using the GRAPPA FF.[2] For the sake of comparison, the minimum in our free-energy profiles for Tyr, Phe, Ile and Leu were -20.8, -14.9, -2.8 and -7.2 kJ mol-1.11m While the different forms of the adsorbates across these two studies (capped amino acids vs. analogues of the side-chain group) prevents any direct comparison of these free energy values, the general agreement between the two studies regarding the aromatic adsorbates was good, with a ratio in the binding energies of Tyr/PhOH:Phe/Bnz to be ~1:1.3). In contrast, a difference is evident for the adsorption of butane and Ile/Leu, which appears relatively weaker using GRAPPA FF, compared with Penna et al. In comparison, Welch et al. also reported Ile and Leu (and Val) to be among the more weakly adsorbing species.[7c] Unfortunately there is a lack of reliable, clear, quantitative experimental data available for comparison, such that the questions regarding the relative strength of adsorption of amino acids cannot be definitively resolved at present.

Multi-Chain Clustering

The two most populated distinct arrangements of each peptide chain in the over-layer were then compared for structural similarity with the six most populated distinct conformations of the adsorbed single peptide chain (Table S6 and S7). As described in the Methods, these six distinct conformations of the single peptide chain were used to build the initial structures of the over-layer. If the root mean squared deviation (RMSD) between the relative position of the peptide backbone atoms of each chain was less than or equal to 2 Å, the conformations (single-chain data *vs.* individual chains in the multi-chain layer) were classified as a 'match' (*i.e.* the peptide backbone conformations were defined to be very similar). We identified several matches for the eight-chain over-layer, indicating that, at this ~50% coverage, there was considerable similarity between the conformational ensemble of the individual chains in the over-layer and those identified for the single-chain system. However, our analysis revealed several new conformations in the over-layer that were not found in the single-chain system. Moreover, for the twelve-chain over-layer we found fewer matches between the conformations of the single chains and those of the chains in the over-layer.

Hydrophobic Inter-chain Contact

Figure S8 shows *g(r)* for the six possible hydrophobic inter-chain residue interactions mediated *via* SD1, and to contrast these results we also provide data for other inter-chain interactions *e.g.* those between Y9-Y9, I1-E5 and Y9-Y12. The strong double peak in the M2-M2 distance distribution indicates interaction between the sulfur atoms of different chains. There was also a peak in the M2-V3 profile and, to a lesser extent, the I1-M2 profile. We suggest that all of these interactions may arise as a result of the sulfur—sulfur non-covalent interaction. In contrast, the I1-I1, I1-V3 and V3-V3 profiles indicated only weak interactions between these residues, and furthermore all of the hydrophobic-hydrophobic interactions between SD1 residues appeared weaker than the interactions between I1-E5, Y9-Y9 and Y9-Y12.

Radius of Gyration Analysis

Figure S9 shows the distribution of the average longitudinal, Rgz, and transverse, Rgt = (Rgx + Rgy)/2, components of the radius of gyration of the GrBP5-WT peptide when adsorbed at the graphene interface for a single chain and for the twelve chain over-layer. The distribution of the two components overlapped to a significant extent, however, the peak of the longitudinal component (located at ~5.5Å) was located at a greater distance than that of the transverse component (~9 Å). In comparing the single-chain case to the over-layer system, there does not appear to be an appreciable change in observed trend, but there is, however, a slight narrowing of the distributions.

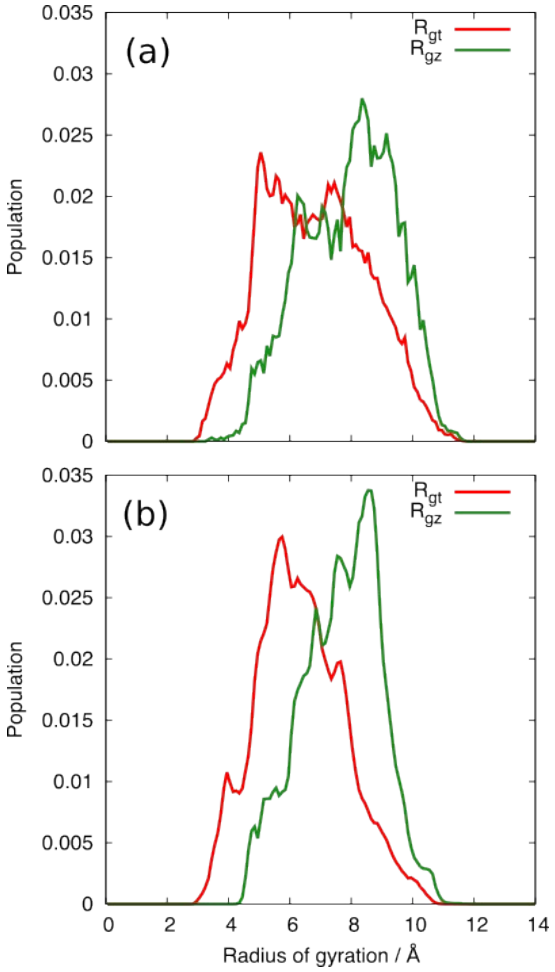

Figure S9: Radius of gyration of the GrBP5-WT peptide chains adsorbed at the aqueous graphene interface, in the lateral and transverse directions, for (a) the single chain and (b) the twelve chain simulations.

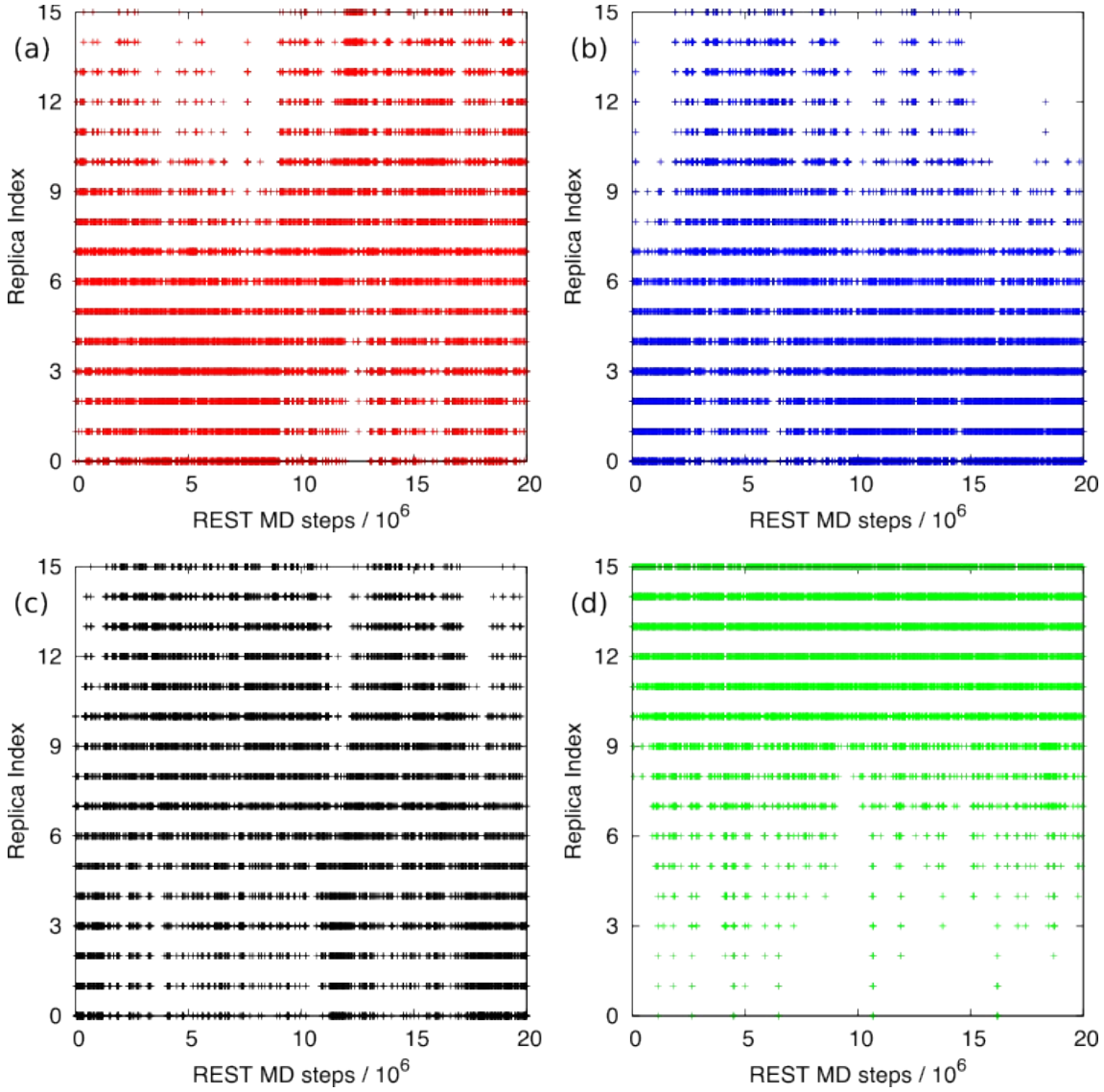

Figure S10: Exemplar REST simulation mobilities in 'effective temperature' space for replicas (a) 0, (b) 5, (c) 10 and (d) 15 of one chain of GrBP5-WT adsorbed at the aqueous graphene interface.

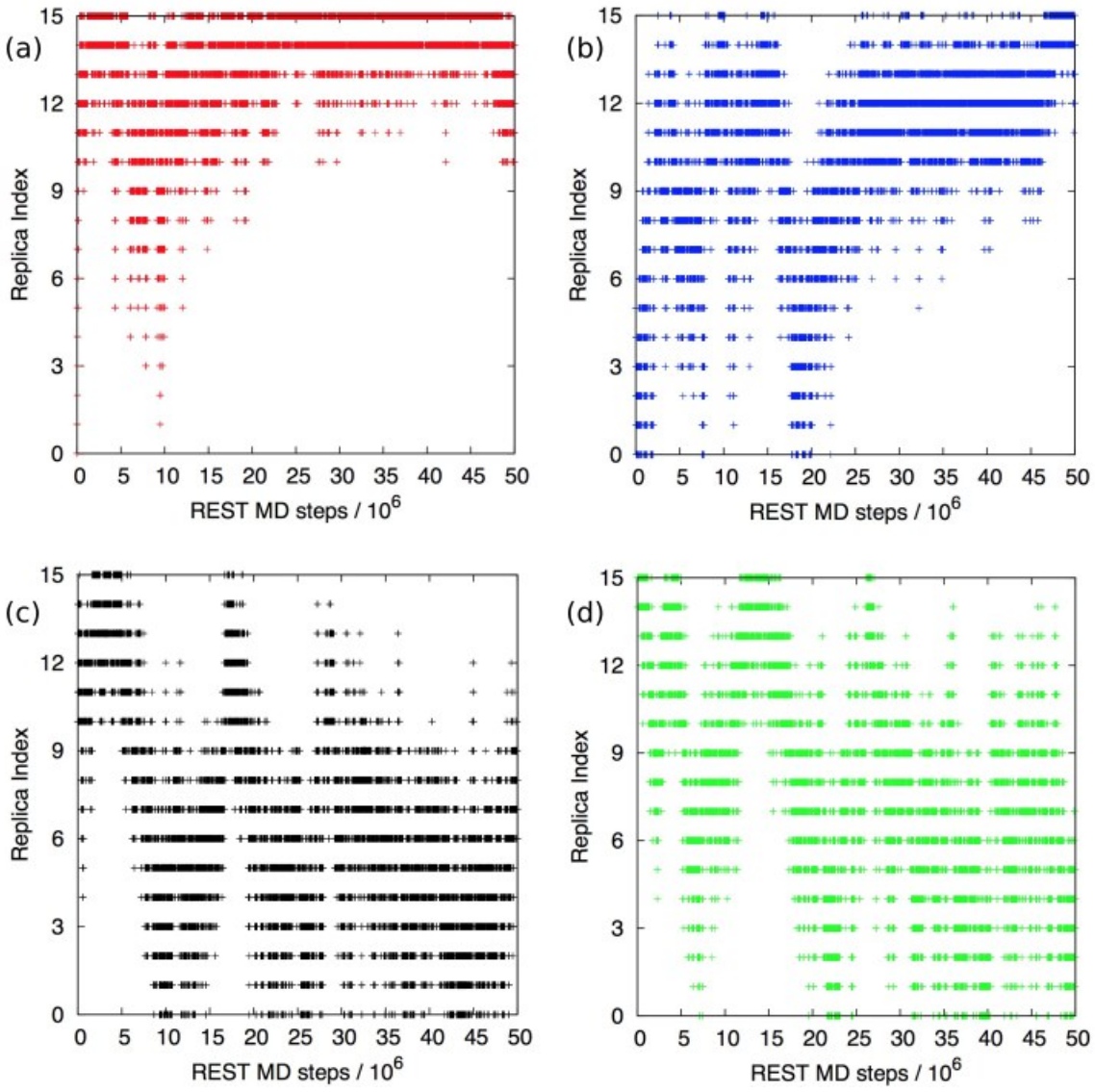

Figure S11: Exemplar REST simulation mobilities in 'effective temperature' space for replicas (a) 0, (b) 5, (c) 10 and (d) 15 of eight chains of GrBP5-WT adsorbed at the aqueous graphene interface.

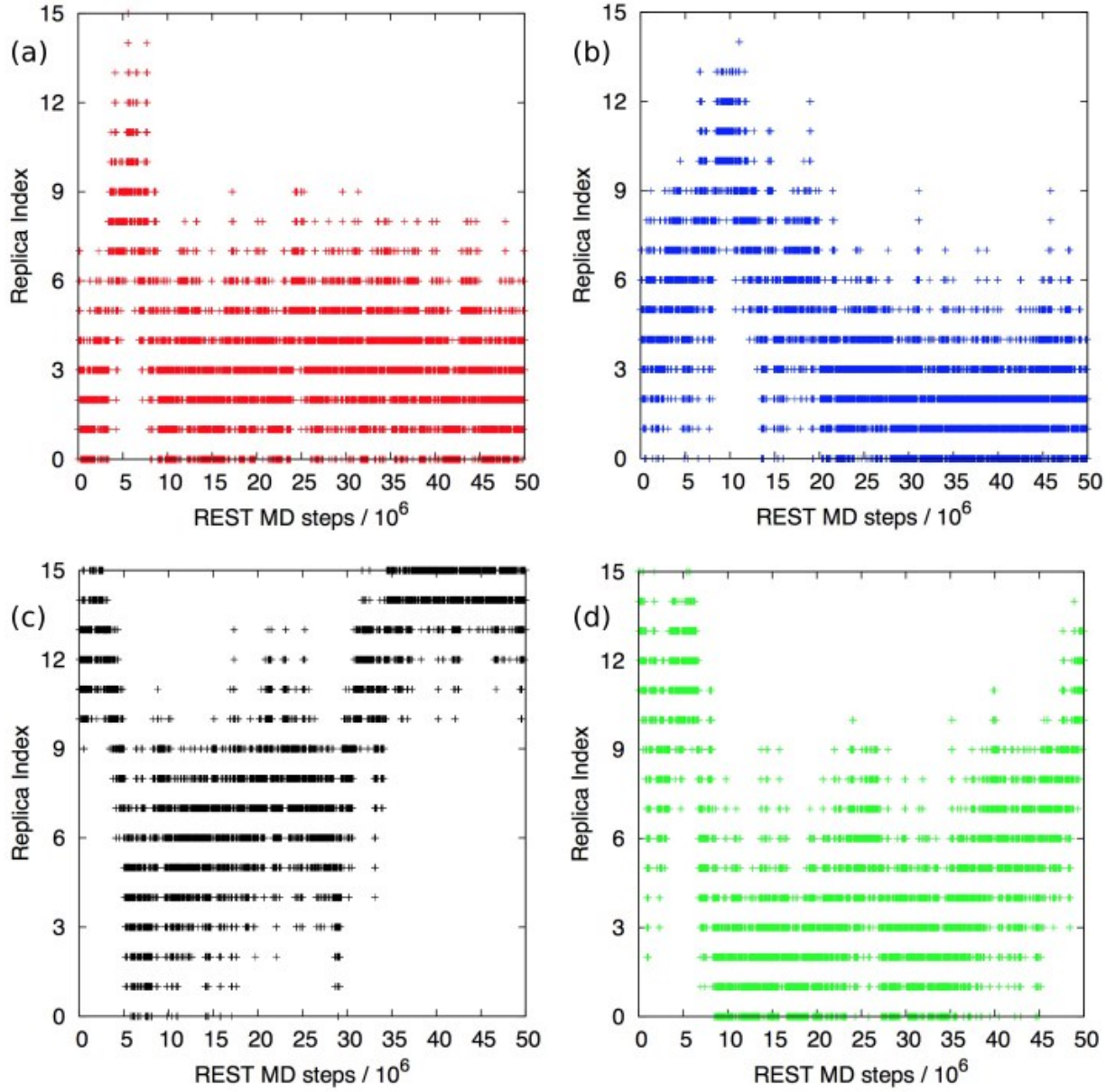

Figure S12: Exemplar REST simulation mobilities in 'effective temperature' space for replicas (a) 0, (b) 5, (c) 10 and (d) 15 of twelve chains of GrBP5-WT adsorbed at the aqueous graphene interface.

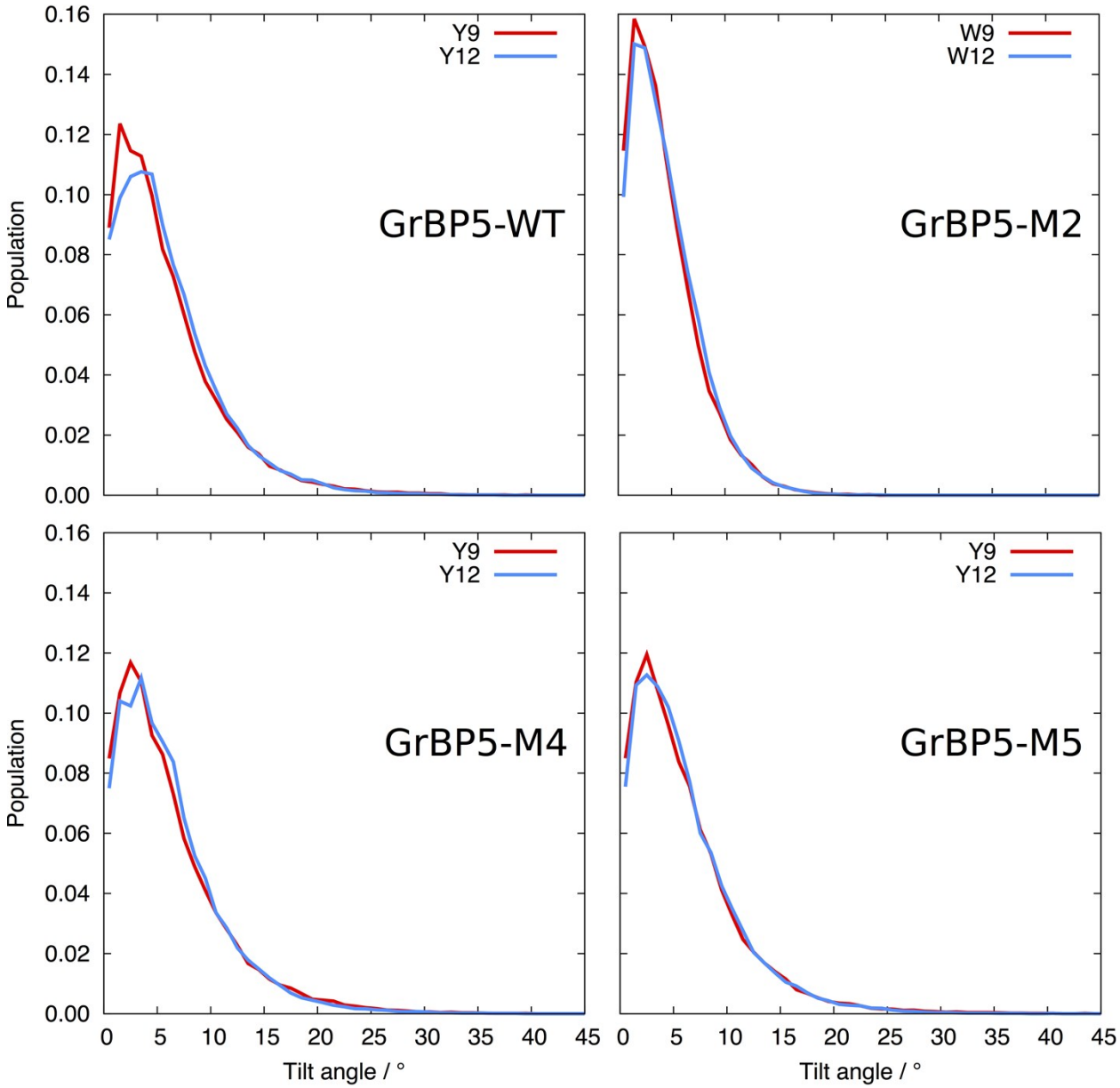

Figure S13: Distribution of ring tilt angle in all four aromatic-containing sequences, calculated from the single-chain REST-MD simulations in the surface-adsorbed state under aqueous conditions. Ring tilt is defined as the angle of the normal of the ring plane with respect to the direction perpendicular to the graphene plane. A tilt angle of zero signifies the ring is in a planar orientation with respect to the graphene surface.

References for Electronic Supplementary Information

[1] M. J. Abraham, T. Murtola, R. Schulz, S. Páll, J. C. Smith, B. Hess and E. Lindahl, *SoftwareX* **2015**, *1-2*, 19.

[2] Z. E. Hughes, S. M. Tomásio and T. R. Walsh, *Nanoscale* **2014**, *6*, 5438.

[3] a) A. D. MacKerell, D. Bashford, M. Bellott, R. L. Dunbrack, J. D. Evanseck, M. J. Field, S. Fischer, J. Gao, H. Guo, S. Ha, D. Joseph-McCarthy, L. Kuchnir, K. Kuczera, F. Lau, C. Mattos, S. Michnick, T. Ngo, D. T. Nguyen, B. Prodhom, W. E. Reiher, B. Roux, M. Schlenkrich, J. C. Smith, R. Stote, J. Straub, M. Watanabe, J. Wiorkiewicz-Kuczera, D. Yin and M. Karplus, *J. Phys. Chem. B* **1998**, *102*, 3586; b) S. Piana, K. Lindorff-Larsen and D. E. Shaw, *Biophys. J.* **2011**, *100*, L47.

[4] a) W. L. Jorgensen, J. Chandrasekhar, J. D. Madura, R. W. Impey and M. L. Klein, *J. Chem. Phys.* **1983**, *79*, 926; b) E. Neria, S. Fischer and M. Karplus, *J. Chem. Phys.* **1996**, *105*, 1902.

[5] T. Darden, D. York and L. Pedersen, *J. Chem. Phys.* **1993**, *98*, 10089.

[6] a) T. Terakawa, T. Kameda and S. Takada, *J. Comput. Chem.* **2010**, *32*, 1228; b) L. B. Wright and T. R. Walsh, *Phys. Chem. Chem. Phys.* **2013**, *15*, 4715.

[7] a) Z. Tang, J. P. Palafox-Hernandez, W.-C. Law, Z. E Hughes, M. T. Swihart, P. N. Prasad, M. R. Knecht and T. R. Walsh, *ACS Nano* **2013**, *7*, 9632; b) A. H. Brown, P. M. Rodger, J. S. Evans and T. R. Walsh, *Biomacromolecules.* **2014**, *15*, 4467. c) Z. E. Hughes and T. R. Walsh, *J. Mater. Chem. B* **2015**, *3*, 3211.

[8] a) W. Hoover, *Phys. Rev., A* **1985**, *31*, 1695-1697; b) S. Nosé, *Mol. Phys.* **1984**, *52*, 255.

[9] X. Daura, K. Gademann, B. Jaun, D. Seebach, W. F. van Gunsteren and A. E. Mark, *Angew. Chem. Int. Ed.* **1999**, *38*, 236.

[10] W. Kabsch and C. Sander, *Biopolymers* **1983**, *22*, 2577.

[11] F. Eisenhaber, P. Lijnzaad, P. Argos, C. Sander and M. Scharf, *J. Comput. Chem.* **1995**, *16*, 273.

[12] M. J. Penna, M. Mijajlovic, C. Tamerler and M. J. Biggs, *Soft Matter*, **2015**, *11*, 5192.